PLASMA HEATING IN PRESENT-DAY AND FUTURE FUSION MACHINES

Yevgen Kazakov, Dirk Van Eester, and Jef Ongena

Laboratory for Plasma Physics, LPP-ERM/KMS,
EUROfusion Consortium Member, Brussels, Belgium

ABSTRACT

A fusion reactor requires plasma pre-heating before the rate of deuterium-tritium fusion reactions becomes significant. Ohmic heating due to the toroidal plasma current that flows in tokamak plasmas allows to reach temperatures of several keV only. In this lecture we provide a short overview of the two main auxiliary heating systems relevant for fusion machines: an injection of high-energy neutral particles and radiofrequency plasma heating.

I. INTRODUCTION

The energy balance for a fusion reactor implies that the energy losses are compensated by the plasma heating due to fusion-born alpha particles. The fusion rate is a strong function of plasma temperature and at low temperatures is negligible. Hence, plasma pre-heating is required before a positive power balance can be reached in a fusion machine.

A fusion triple product, which characterizes the performance of a fusion device, is minimized at plasma temperature $T \approx 15$ keV. The initial heating in tokamaks comes from the ohmic heating: likewise an electric current flowing through a metal wire heats it up, the toroidal plasma current, which is used in tokamaks for plasma confinement, dissipates its energy and heats the plasma. However, ohmic heating allows to reach plasma temperature of a few keV only [1, 2]. As the plasma temperature increases, the collisional frequency and the plasma resistivity, being proportional to $\propto 1/T^{3/2}$, decrease. The limitations of ohmic heating are discussed in more detail in a separate lecture by R. Koch and D. Van Eester [3]. There, it is also shown that raising the plasma current to increase the ohmic power $P_\Omega = R\, I_{\rm pl}^2$ is limited by the necessity to keep the edge safety factor $q_{\rm edge} > 2$ for MHD stability of the plasma. Note that for stellarators the confining magnetic field is solely produced by the external magnetic coils and the plasma current is so low that ohmic heating is negligible.

There are two main methods for heating fusion plasmas. The first technique is based on injecting the beam of high-energy neutral particles to the plasma (NBI). As the beam particles are ionized in the plasma, they transfer their energy to bulk ions and electrons via Coulomb collisions. The second method relies on launching electromagnetic waves into the plasma and providing proper conditions for strong localized wave damping by ions and/or electrons. Due to the inhomogeneity of the confining magnetic field in toroidal plasmas, the position of the power deposition for radiofrequency (RF) heating can be controlled externally, e.g., by a choice of the wave frequency. The supported by plasmas resonant wave frequencies will be identified below, using a simplified – yet, good as a first approximation – cold-plasma approach.

There are numerous applications of NBI and RF systems beyond heating itself. Tokamaks are inherently pulsed machines, and driving non-inductive current with auxiliary heating systems is essential for maximizing the plasma pulse duration, a prerequisite condition for economic viability of tokamaks as fusion reactors. Heating systems are also routinely used for diagnostics purposes, controlling impurities and plasma instabilities, optimizing particle and energy transport, for plasma start-up and landing, etc.

II. NEUTRAL BEAM INJECTION HEATING

Neutral beam injection has been used as a working horse for plasma heating in most of fusion machines. For instance, the world highest fusion power 16 MW was obtained on JET tokamak by injecting 22 MW of NBI and 3 MW of ICRF heating. A strong magnetic field is used for plasma confinement in magnetic fusion devices, and this prohibits a direct injection of energetic ions into the plasma. Whereas injected energetic ions will be deflected by the magnetic field and can not penetrate deep into the plasma, neutral particles do not feel the Lorentz force and will travel along straight-line trajectories until their ionization by collisions with the background plasma. The penetration length for a beam in the plasma – before most of its power is deposited due to ionization – depends essentially on the injection beam energy $E_{\rm NBI}$. As will be discussed in this section, most of present-day tokamaks and stellarators operate with beam energies $E_{\rm NBI} \simeq 100$ keV, and the application of NBI to

ITER and next-step devices requires a fundamental change and an increase of the beam energy by an order of magnitude up to $E_{\rm NBI} \simeq 1$ MeV. $E_{\rm NBI}$ also determines whether a collisional ion or electron heating dominates due to the slowing down of the NBI-generated fast ions. Present-day NBI systems usually provide a high fraction of ion heating, while for the future machines most of the injected beam power will be transferred to electrons.

A schematic diagram of NBI system is shown in Fig. 1. There is no direct way of accelerating neutral particles to high energies, and one still has to start with accelerating electrically charged ions, and then set a dedicated system to convert energetic ions into energetic neutral particles. Low-energy ion source is a first step of the NBI system. Beam energies of about 100 keV are sufficient for the machine's and plasma parameters of the existing fusion devices, and this allows using well-established techniques for producing positive ions. However, ion sources based on a plasma discharge produce not only the required atomic ions (e.g., D^+), but also a significant fraction of molecular ions (D_2^+ and D_3^+). The molecular ions will ultimately dissociate into atoms with one-half and one-third NBI energies. Such $E_{\rm NBI}/2$ and $E_{\rm NBI}/3$ atoms will have a lower penetration to the plasma and deposit more heating at the plasma edge, which is not desirable. In future fusion machines, including ITER, a different technology for the ion source has to be adopted, and NBI systems will be based on using negative ion beams (N-NBI).

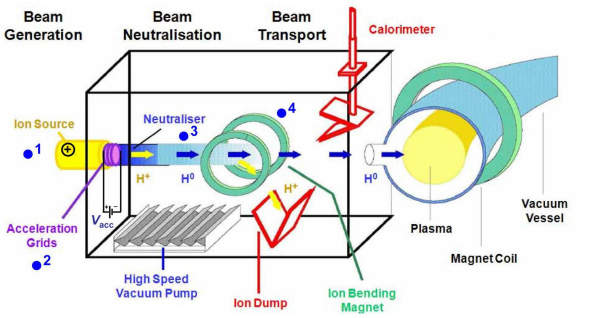

Figure 1: Layout of neutral beam injection system (Courtesy: Ursel Fantz, IPP-Garching).

At the second stage, the ions are accelerated to the required energy by applying a high DC voltage. Because a positive electrostatic voltage will be applied to extract negative ions in N-NBI systems, there will be no one-half and one-third beam components present after the extraction. The accelerated beam current is usually about 50 A, and one can easily compute the consumed input electrical power for this part of NBI system by multiplying the acceleration voltage by the beam current.

After this stage a directed beam of high-energy ions is formed and it enters the neutralization chamber, where the conversion of energetic ions into energetic neutrals occurs. The neutralizer consists of a simple gas cell, filled with the molecular gas and open at each end, through which the beam passes. Normally the gas species for the neutralizer is chosen the same as for the ion source. The density of the neutralizing gas is varied to achieve the maximum efficiency of ion-to-neutral conversion. Figure 2 depicts the maximum neutralization efficiency, $\eta_{\rm neutr.}^{\rm (max)}$ computed for atomic D and H ion beams as a function of beam energy. For the same NBI acceleration energy, the neutralization efficiency of H beams is lower than for D beams because of the larger energy per nucleon. As follows from this figure, the neutralization efficiency for D^+ ions at $E_{\rm NBI} \approx 100$ keV is reasonably good, $\approx 50\%$, but at higher beam energies decreases to unacceptably low levels. In contrast, for negative beams (both for D^- and H^-) the neutralization efficiency is much higher, $\eta_{\rm neutr.}^{\rm (max)} \approx 60\%$. This is the reason why using negative ions is the inevitable choice for neutral beam systems of ITER and future fusion machines, which will operate at MeV level.

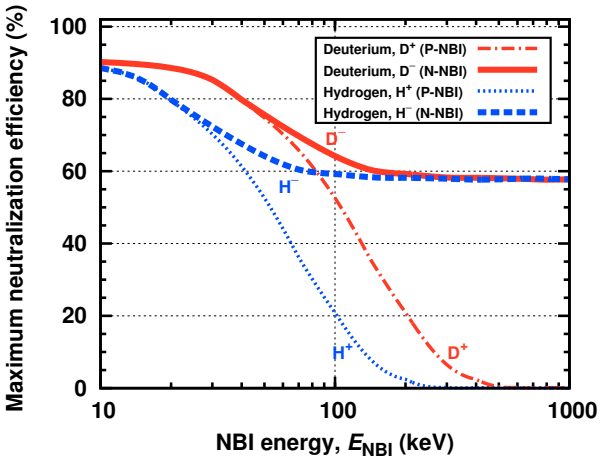

Figure 2: Maximum neutralization efficiency for D and H atomic ion beams as a function of beam energy.

It is quite easy to compute quantitatively the maximum value of $\eta_{\rm neutr.}$ for N-NBI systems. At high beam energies $200 - 1000$ keV/amu, the two most important reactions occurring in the neutralizer are: 1) a stripping reaction $D^- + D_2 \rightarrow D_0 + D_2 + e$ (cross-section σ_{-10}), which converts a negative ion to an energetic neutral; and 2) a competing loss process due to a re-ionization of the formed neutral by a collision with background neutrals, $D_0 + D_2 \rightarrow D^+ + D_2 + e$ (σ_{01}). Also negative ions can be directly converted to positive ions via a reaction $D^- + D_2 \rightarrow D^+ + D_2 + 2e$ (cross-section σ_{-11}). Then, the maximum neutralization efficiency, when the gas density of the neutralizer is optimized for D^0 generation, is connected to the cross-sections as follows

$$\eta_{\rm neutr.}^{\rm (max)} = \frac{\sigma_{-10}}{\sigma_{-10} + \sigma_{-11}}\, p^{p/(1-p)} \approx 58\%. \qquad (1)$$

Here, $p = \sigma_{01}/(\sigma_{-10} + \sigma_{-11}) \approx 0.28$ and the first term $\sigma_{-10}/(\sigma_{-10} + \sigma_{-11}) \approx 0.95$. The tabulated data for the cross-sections can be found in [4]. For negative ions the neutralization efficiency at high beam energies remains nearly constant. At the exit of the neutralizer, the beam consists of 58% of high-energy neutrals, and 25% and 17% of positive and negative ions, respectively.

One should note here that for present-day NBI systems based on positive ions, the acceleration energy, beam current and beam power fractions depend significantly on the ion species used for injection. Table 1 illustrates this for the NBI system of the tokamak JET, which consists of two neutral injector boxes equipped each with up to eight positive ion neutral injectors (PINIs) [5]. The system was recently upgraded to increase the total injected deuterium neutral beam power to at least 34 MW and to increase the beam pulse length. If operating with deuterium, the full-energy beam component carries about 50% of the total NBI power, and for the hydrogen mode of operation a half-energy component is the dominant.

Table 1: Measured (D_2) and predicted (H_2 and T_2) parameters of the JET NBI system after the completion of recent upgrade [5]. The total power is computed for two neutral injector boxes equipped with up to eight PINIs each.

Parameter \ Gas species	H_2	D_2	T_2
Max. beam energy (keV)	90	125	118
Max. beam current (A)	50	65	45
Max. power per PINI (MW)	1.0	2.16	2.2
Max. total power (MW)	16.0	34.6	35.2
Predicted beam power fractions, $E_0 : E_0/2 : E_0/3$	28:44:28	52:39:9	63:26:11

Since one should avoid of injecting high-energy positive/negative ions from NBI system to the plasma (after entering the plasma they will likely deposit their energy on the neutral beam entrance port), the next stage of the NBI system is the residual ion dump. Here, the charged beam components are filtered out by using the deflection magnets or the electrostatic field. To increase the wall-plug efficiency of NBI systems (in present-day machines it is $\approx 20 - 30\%$ only), for devices following ITER a possibility of energy recovery (recirculating the residual negative ions) is explored [6]. In addition, utilizing photo-detachment or plasma neutralizers to improve the neutralization efficiency beyond 58% – maximum for the standard gas neutralizers – is being actively studied in the context of DEMO development. The wall-plug efficiency of NBI systems has to be improved by a factor of two to become reactor-relevant [6].

After passing the neutralization stage, the remaining neutral beam either impinges onto the calorimeter or continues into the duct leading to a plasma. Adopting a movable calorimeter allows an off-line commissioning and optimization of the beam system without plasma operation. Combined with measurements of the losses in the neutral beam duct, this also allows the injected NBI power to be determined independently of the plasma device.

Estimating the required NBI energy

In this subsection, we estimate the required beam energies as a function of machine's size and operational plasma densities, and show why NBI system for ITER has to provide beams with the energy of about 1 MeV.

When the neutral beam particles enter the plasma, there are several processes causing an ionization of a high-energy neutral in a plasma: charge exchange, electron and ion impact ionization in collisions with plasma electrons, ions and impurities. As the neutral beam penetrates and is absorbed in the plasma, its flux exponentially decays with the propagation distance, $I(\Delta l) = I_0 \exp[-\int_0^{\Delta l} dl\, n(\vec{r})\sigma(\vec{r})]$, where Δl is a distance along the beam propagation path. Assuming a constant density profile $n \approx$ const, one can write

$$I(\Delta l) = I_0 e^{-\Delta l / L_{\rm NBI}}. \qquad (2)$$

A characteristic distance, at which the initial beam intensity is attenuated by a factor of $e \approx 2.7$ – further referred to as the beam decay length – is then $L_{\rm NBI} = 1/(n\sigma)$. For simplicity, we neglect an ionization due to electron impact. For $E/A_{\rm NBI} \geq 40$ keV/amu, the total cross-section for charge exchange and ion impact is inversely proportional to the beam energy and can be approximated as $\sigma_{i+\rm CX}(\rm m^2) \approx 1.8 \times 10^{-18} / [E_{\rm NBI}(\rm keV)/A_{\rm NBI}]$. Then, the beam decay length is given by

$$L_{\rm NBI}(\rm m)|_{\sigma=\sigma_{\rm CX}+\sigma_i} \simeq \frac{E_{\rm NBI}(\rm keV)/A_{\rm NBI}}{180 n_{e,20}}, \qquad (3)$$

where $n_{e,20}$ is the plasma density expressed in the units 10^{20} $\rm m^{-3}$.

Let us consider an updated JET NBI system with 125 keV D^0 beams as an example. Using a typical plasma density of $n_e = 5 \times 10^{19}$ $\rm m^{-3}$, Eq. (3) predicts $L_{\rm NBI} \approx 0.7$ m, which is comparable to the minor radius of the machine $a \approx 0.9$ m. However, such NBI energies are too low for heating ITER plasmas ($a = 2$ m, $n_e = 1 \times 10^{20}$ $\rm m^{-3}$): according to Eq. (3), at $E_{\rm NBI} = 125$ keV a decay length will be $L_{\rm NBI} \approx 0.35$ m (taking into account charge-exchange and ion impact ionization mechanisms only). A short decay length (i.e., $L_{\rm NBI} \ll a$) is undesirable since most of the energy is deposited at the outer part of the plasma volume. As a result, the beam energy has to be significantly increased for ITER and future

larger, higher-density fusion machines in order to allow neutrals to penetrate deeper into the plasma.

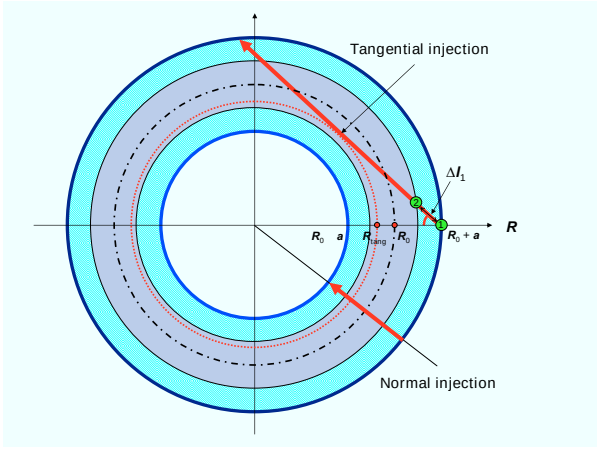

Figure 3: Plan view illustrating a very different beam propagation length for normal and tangential NBI injection.

The required NBI energy for ITER can be estimated as follows (see Fig. 3). In ITER, the two heating neutral beams will inject beams tangentially with a tangency radius $R_{\rm tang} = 5.28$ m ($R_{\rm tang} \approx R_0 - a/2$), and the third diagnostic beam is designed for a normal injection [7]. The full path of the tangential beam through the plasma is $\Delta l_2 = 2\sqrt{(R_0+a)^2 - R_{\rm tang}^2} \approx 12.5$ m, and because of the very long geometrical distance the shinethrough fraction (amount of NBI power arriving at the wall) is very small. However, a significant fraction of beam power is deposited in the outer shell of the plasma during a relatively short path of the beam since its entrance to the plasma (point '1' in Fig. 3) to the point, when it intersects the flux surface $r/a = 0.5$ (point '2'). This distance is given by $\Delta l_1 = \sqrt{(R_0+a)^2 - R_{\rm tang}^2} - \sqrt{(R_0+a/2)^2 - R_{\rm tang}^2} \approx 1.4$ m. The fraction of beam power deposited along this path is $p_{\rm abs} \approx 1 - {\rm e}^{-\Delta l_1/L_{\rm NBI}}$, and this sets a limitation on the acceptable NBI decay length and, hence, required beam energies. $L_{\rm NBI}$ should be comparable to Δl_1 or even less in order to reduce the beam power deposition at the edge. In fact, already at $\Delta l_1/L_{\rm NBI} = 0.7$, $> 50\%$ of the incident beam power is deposited within $r/a \geq 0.5$ region. For a fusion device with the ITER-like aspect ratio, Δl_1 can be approximated as $\sqrt{aR_0}/3$, and one can derive an estimate for the required NBI energy ($L_{\rm NBI} \gtrsim 0.5\sqrt{aR_0}$)

$$E_{\rm NBI}({\rm keV})|_{\sigma=\sigma_{\rm CX}+\sigma_i} \gtrsim 90\,\sqrt{aR_0}\,n_{e,20}\,A_{\rm NBI}. \quad (4)$$

In Eq. (4), the beam energy is given in keV, and the machine's minor and major radii are in meters.

For ITER operating with deuterium beams, Eq. (4) yields an estimate of $E_{\rm NBI} \approx 600$ keV. Why are then heating NBI systems of ITER designed for 1 MeV D_0 beams? In fact, at high beam energies (of several hundreds keV or higher) an additional mechanism – multistep ionization – produces a substantial increase of the beam stopping cross-section and this reduces the beam penetration. As discussed in [8, 9], the multistep ionization arises from excitation of the beams and the subsequent ionization of already excited neutral atoms. The enhancement factor of the ionization against the single step-processes considered above, $\sigma_{\rm eff} = \sigma(1+\delta)$ is theoretically predicted to increase with the beam energy and the electron density, $\delta = \delta(E_{\rm NBI}, n_e, ...)$. While an effect of the multistep ionization is relatively small for present-day beam systems, an enhancement of the stopping cross-section by a factor of two was measured for 350 keV hydrogen beam in JT-60U tokamak ($\delta \approx 0.8 - 1.05$), in accordance with theoretical predictions. A similar enhancement factor is expected for high-energy deuterium beams in ITER. Then, Eq. (3) for estimating the beam decay length in a plasma has to be adopted accordingly to include the multistep ionization

$$L_{\rm NBI}({\rm m}) \simeq \frac{E_{\rm NBI}({\rm keV})/A_{\rm NBI}}{180\,(1+\delta)\,n_{e,20}}. \quad (5)$$

The same multiplication factor $(1+\delta)$ has to be included to Eq. (4), when estimating the required beam energies and this correction yields $E_{\rm NBI} \approx 1$ MeV for ITER.

Initially ITER will use two neutral beams for plasma heating that are designed to inject each 16.5 MW of power to the plasma. Operation with deuterium (1 MeV/40 A) and hydrogen (870 keV/46 A) will be supported. Note that whereas tritium has been used with positive ion based injectors during the D-T experiments on JET and TFTR tokamaks, a current status of the ITER NBI design does not consider using tritium due to the regulations on tritium handling. The third NBI port in ITER is reserved for the diagnostics neutral beam that will be installed to support the charge exchange recombination spectroscopy, which is an essential diagnostic for the measurement of the helium-ash density in the core of D-T plasmas. The diagnostics neutral beam in ITER will use a normal injection of the hydrogen beam with a much smaller energy (H^-, 100 keV/60 A).

Critical energy

After the ionization of the injected neutral particles in the plasma, the resulting fast ions are slowed down by Coulomb collisions with bulk plasma ions and electrons. A Fokker-Planck description of the test-particle slowing down is normally adopted to compute the resulting power deposition. The

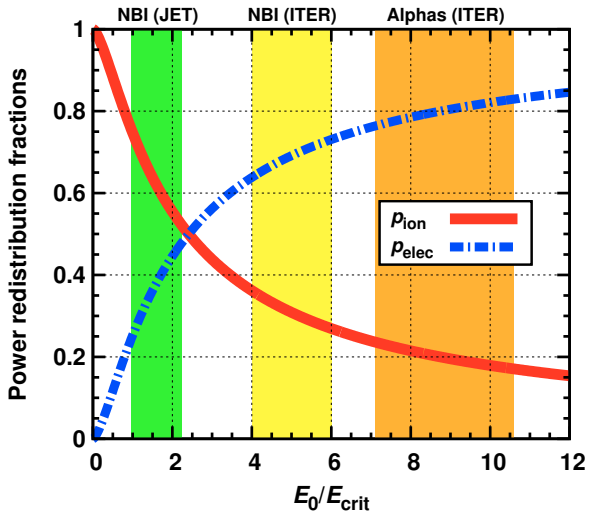

Figure 4: Fraction of the fast ion energy transferred to bulk ions and to electrons as a function of $E_0/E_{\rm crit}$. The shaded areas highlight regimes relevant for JET NBI system ($E_0^{(\rm D)}$=125 keV, $T = 3-7$ keV), ITER N-NBI system ($E_0^{(\rm D)} = 1$ MeV, $T = 10-15$ keV), and for fusion-born alpha particles ($E_0^{(\alpha)} = 3.5$ MeV).

corresponding derivation one can find in a lecture [3]. For our discussion it is sufficient to note that whether the resultant dominant bulk ion or electron heating occurs, depends on the ratio of the fast-particle energy to the so-called critical energy, $E_{\rm crit}$ defined as

$$E_{\rm crit} = 14.8 A_{\rm fast} T_e \left(\sum_i X_i Z_i^2 / A_i \right)^{2/3}, \qquad (6)$$

where $X_i = n_i/n_e$ are the concentrations of various ion species in a plasma. A fast ion with the energy $E = E_{\rm crit}$, transfers instantaneously the same amount of power to ions and electrons via collisions.

If we consider a slowing down of fast particles with the initial (birth) energy E_0 to thermal velocities, then the average fraction of the total energy given up by the fast particles, which goes into the thermal bulk ions of the plasma, is

$$p_i(E_0) = \frac{E_{\rm crit}}{E_0} \int_0^{E_0/E_{\rm crit}} \frac{dy}{1+y^{3/2}}. \qquad (7)$$

The fraction of power flowing to electrons is then

$$p_e(E_0) = 1 - p_i(E_0). \qquad (8)$$

A plot of p_i and p_e as a function of $E_0/E_{\rm crit}$ is shown in Fig. 4. Note that at $E_0 = E_{\rm crit}$ about 75% of the fast ion energy is transferred to the plasma ions, and an equal total energy transfer to ions and electrons is reached at $E_0/E_{\rm crit} \approx 2.4$.

It is instructive to illustrate these results with a few examples. For $E_{\rm NBI}^{(\rm D)} = 125$ keV beam particles injected to 5 keV deuterium plasma, $E_0/E_{\rm crit} \approx 1.3$ and p_i:$p_e \approx$ 2:1. For NBI system relevant for ITER a much higher beam energy has to be adopted, as discussed in the previous subsection, and the ratio $E_0/E_{\rm crit}$ will be significantly larger than for the present-day NBI systems. As a result, N-NBI systems with $E_{\rm NBI} \approx 1$ MeV will provide a dominant electron heating. A similar test-particle slowing down reasoning applies for fusion-born alpha particles. Since the birth energy of alpha particles is 3.5 MeV, this means that their energy loss is mainly due to collisions with plasma electrons.

III. RADIOFREQUENCY HEATING

Radiofrequency heating is another very efficient method for increasing fusion plasma temperatures. Magnetized plasmas have several 'natural' resonant frequencies and support the variety of wave modes. This results in the existence of many different RF heating and current drive scenarios. Though RF heating involves a much more complicated physics of electromagnetic wave propagation in plasmas and wave-particle interaction, this, in turn, makes RF heating much more flexible in terms of external control of the heating region than for neutral beams. For example, if the RF heating in the ion cyclotron range of frequencies (ICRF) is applied, changing power deposition from dominant ion to dominant electron can be done by varying the chosen operational wave frequency or selecting a proper plasma composition. Furthermore, ICRF is the only heating method in future fusion machines capable of providing a significant fraction of bulk ion heating. On the other hand, heating in the electron cyclotron range of frequencies (ECRF) is characterized with a very localized power deposition, and this allows also to use ECRF as a tool to control the plasma pressure and current density profiles for the MHD plasma stability [10]. Lower hybrid (LH) heating has been actively exploited on different present-day machines as a very efficient method of non-inductive current drive.

For ITER, in addition to 33 MW of NBI power, installing two RF heating systems (ECRH and ICRH) each providing 20 MW of auxiliary power is foreseen. A further 40 MW upgrade of the ITER heating mix, with a possibility of installing lower hybrid heating, is also considered.

The principle of wave heating is similar for all RF scenarios. A generator (the type of utilized source is very different depending on the operating frequency) sends waves along the transmission line to a launching structure located at the plasma edge [11]. Then, in contrast to NBI heating which has no problem of injecting neutral particles to the plasma, a special care has to be taken to optimize coupling of RF power from the launcher to the plasma [12]. Once the required electromagnetic wave starts its propagation in the plasma, the focus of the discussion shifts

towards understanding how to make RF power to be absorbed at a desired part of the plasma volume, often preferably close to the plasma center.

It is impossible to cover all aspects of plasma waves physics in a short lecture note. An interested reader is referred to lectures [13, 14] for the further reading, and to books [15, 16] for an in-depth discussion on plasma waves in magnetized plasmas. In this lecture note, we will focus only on a single issue of RF plasma heating: determining resonant wave frequencies suitable for efficient heating and current drive.

Cold plasma dielectric tensor

The propagation of electromagnetic waves in an arbitrary medium is described by Maxwell's equations (cgs system is adopted here)

$$\begin{cases} \mathrm{rot}\vec{E} = -\dfrac{1}{c}\dfrac{\partial \vec{B}}{\partial t} \\ \mathrm{rot}\vec{B} = \dfrac{1}{c}\dfrac{\partial \vec{E}}{\partial t} + \dfrac{4\pi}{c}\vec{j}. \end{cases} \tag{9}$$

Plasma consists of charged particles, ions and electrons, and it influences the wave propagation characteristics via the wave induced current density $\vec{j}$. Depending on the level of complexity of describing the system, different plasma models can be adopted. We consider the simplest case, when a cold plasma is immersed in a constant equilibrium magnetic field $\vec{B} = B_0\vec{e}_z$ and the wave amplitude is small such that wave propagation can be treated as a linearized perturbation for every individual mode $\vec{B}_\sim, \vec{E}_\sim \propto e^{i(\vec{k}\vec{r}-\omega t)}$ (ω is the wave frequency and $\vec{k}$ is the wave number). Under these assumptions, the time derivative and curl operator in Eqs. (9) can be replaced with $\partial/\partial t \to -i\omega$ and $\mathrm{rot} = i\vec{k}\times$, respectively.

Cold plasma description allows to use a simple equation of motion for an ion/electron, $d\vec{v}/dt = q\vec{E}/m + (qB_0/mc)\,\vec{v}\times\vec{e}_z$, to characterize its response to the electromagnetic field. This equation for the simplified case considered here can be easily solved, and the individual velocity components as a function of RF electric field are given by

$$\begin{cases} v_x = \dfrac{iq}{m}\dfrac{\omega}{\omega^2-\omega_c^2}E_x - \dfrac{q}{m}\dfrac{\omega_c}{\omega^2-\omega_c^2}E_y, \\ v_y = \dfrac{iq}{m}\dfrac{\omega}{\omega^2-\omega_c^2}E_y + \dfrac{q}{m}\dfrac{\omega_c}{\omega^2-\omega_c^2}E_x, \\ v_z = \dfrac{iq}{m\omega}E_z, \end{cases} \tag{10}$$

and the cyclotron frequency $\omega_c = qB_0/mc$ has been introduced. The cyclotron frequency depends on q/m ratio of a particle, and therefore for electrons it is about 2000 times larger than for ions. In addition, ω_c includes the sign of a particle's charge, which reflects the fact that ions and electrons rotate in the opposite directions around the confining magnetic field. As follows from Eq. (10), if $B_0 \neq 0$ plasma behaves as a gyrotropic medium: e.g., v_x component is not only proportional to E_x, but depends also on E_y.

If v_i as a function of $\vec{E}$ are known, the current density can be easily computed $\vec{j} = \sum_{s=e,i} q_s n_s \vec{v}_s$ and formally written as $\vec{j} = \overline{\overline{\sigma}}\vec{E}$ ($\overline{\overline{\sigma}}$ is defined as the conductivity tensor). The second equation (9) is often re-written in a simpler form, by combining the two terms at the right-hand side

$$\mathrm{rot}\vec{B} = \frac{1}{c}\frac{\partial \vec{E}}{\partial t} + \frac{4\pi}{c}\vec{j} = \frac{1}{c}\frac{\partial(\overline{\overline{\epsilon}}\vec{E})}{\partial t}, \tag{11}$$

and introducing a quantity $\overline{\overline{\epsilon}}$, which is called as the plasma dielectric tensor. The plasma dielectric and the conductivity tensors are related via $\overline{\overline{\epsilon}} = \overline{\overline{I}} + (4\pi i/\omega)\overline{\overline{\sigma}}$.

Then, by introducing the wave refractive index $\vec{n} = c\vec{k}/\omega$, Eqs. (9) and (11) can be merged into a single equation for the RF electric field $\vec{E}$

$$\vec{n}\times(\vec{n}\times\vec{E}) + \overline{\overline{\epsilon}}\vec{E} = 0. \tag{12}$$

In the cold plasma limit, the plasma dielectric tensor is a function of the imposed wave frequency (see Eqs. (10)), but is independent of the wave number. The Stix's notation for $\overline{\overline{\epsilon}}$ is commonly adopted [15]

$$\overline{\overline{\epsilon}} = \overline{\overline{\epsilon}}(\omega) = \begin{pmatrix} S & -iD & 0 \\ +iD & S & 0 \\ 0 & 0 & P \end{pmatrix}, \tag{13}$$

where $S(\omega) = 1 - \sum_s \omega_{ps}^2/(\omega^2-\omega_{cs}^2)$, $D(\omega) = \sum_s(\omega_{cs}/\omega)(\omega_{ps}^2/(\omega^2-\omega_{cs}^2))$, $P(\omega) = 1 - \sum_s \omega_{ps}^2/\omega^2$, and $\omega_{ps}^2 = 4\pi n_s q_s^2/m_s$ is the square of the plasma frequency.

Equation (12) is a set of three coupled, linear, homogeneous equations for the three components of the RF electric field. Requiring non-trivial solutions to exist, the determinant of these equations must vanish, and one can obtain the wave dispersion relation, which defines the refractive index n as a function of wave frequency ω:

$$A(\omega,\theta)n^4 - B(\omega,\theta)n^2 + C(\omega,\theta) = 0, \tag{14}$$

where θ is an angle between the wave vector and the confining magnetic field ($k_y = 0$), and the functions $A(\omega,\theta), B(\omega,\theta)$ and $C(\omega,\theta)$ can be easily derived (see, e.g., [15]).

Equation (14) is a bi-quadratic, and hence for any ω there are two – generally different – solutions $n^2 = n_{1,2}^2(\omega)$. This means that within the cold plasma approximation for any wave frequency plasma supports two different wave modes (with a different dispersion relation). In hot plasmas, the dielectric tensor is also a function of the wave number $\vec{k}$, which leads to the appearance of extra new modes and solutions, and makes wave physics more complicated.

For heating fusion plasmas, the electromagnetic waves are usually excited to propagate predominantly perpendicular to the confining magnetic field. For a simplified limiting case of purely perpendicular propagation $\theta = \pi/2$, the wave resonances are determined by the condition

$$A(\omega, \theta = \pi/2) = S(\omega) = 1 - \sum_{s=e,i} \frac{\omega_{ps}^2}{\omega^2 - \omega_{cs}^2} = 0. \quad (15)$$

This is a desired equation for computing the resonant wave frequencies (for a perpendicular, cold plasma resonance). The solutions of Eq. (15) define the range of electromagnetic frequencies used for efficient plasma heating and current drive in fusion plasmas.

Resonant wave frequencies

Before we proceed to finding solutions of Eq. (15), it is helpful to note that the electron plasma and electron cyclotron frequencies are comparable in the core of fusion plasmas ($\omega_{pe}/\omega_{ce} \approx 3\sqrt{n_{e,20}}/B_\mathrm{T}$; B_T is the confining magnetic field in Tesla), and the relation $\omega_{pi}^2/\omega_{ci}^2 \gg 1$ holds for bulk ions. Another useful identity is $\omega_{pe}^2/|\omega_{ce}| = \sum_i \omega_{pi}^2/\omega_{ci}$ – this is just the charge quasi-neutrality re-written in a different way.

1) ECRF (electron cyclotron range of frequencies), $f \simeq f_{ce} \gg f_{ci}$.

For this frequency range ions are immobile and Eq. (15) can be simplified by neglecting the ion contribution term ($\simeq \omega_{pi}^2/\omega_{ce}^2 \propto m_e/m_i \ll 1$)

$$S(\omega) = 1 - \cancel{\sum_i \frac{\omega_{pi}^2}{\omega^2 - \omega_{ci}^2}} - \frac{\omega_{pe}^2}{\omega^2 - \omega_{ce}^2} = 0. \quad (16)$$

This defines the resonant frequency known as the upper hybrid (UH) resonance

$$\omega_\mathrm{UH}^2 = \omega_{ce}^2 + \omega_{pe}^2. \quad (17)$$

The word 'hybrid' refers here that the resonant frequency involves both ω_{ce} and ω_{pe}. The upper hybrid frequency is somewhat above ω_{ce}. Since $f_{ce} \approx 28 \times 10^9\, B_\mathrm{T}$, ECRF heating requires sources in the range 100–200 GHz. Note that gyrotrons – sources for ECRF heating – can deliver one or a few wave frequencies only. For ITER, $f = 170$ GHz is selected and the radiofrequency sources for the ECRF system will be composed of 24 gyrotrons (with 1 MW unit output).

2) ICRF (ion cyclotron range of frequencies), $f \simeq f_{ci} \ll f_{ce}$.

For this frequency range, a resonant frequency occurs when there are two or more ion species present in a plasma

$$S(\omega) = \cancel{1} - \frac{\omega_{p1}^2}{\omega^2 - \omega_{c1}^2} - \frac{\omega_{p2}^2}{\omega^2 - \omega_{c2}^2} - \cancel{\frac{\omega_{pe}^2}{\omega^2 - \omega_{ce}^2}} = 0. \quad (18)$$

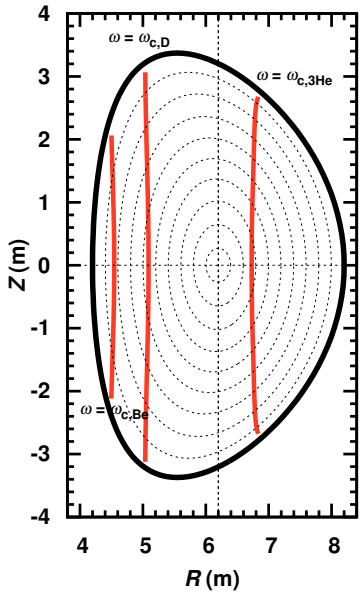

Figure 5: Location of ion cyclotron resonance layers in ITER-like plasma for $f = 50$ MHz ($B_0 = 5.3$ T).

Then, the vacuum and electron contributions are negligible in comparison with the contributions due to ion species, which balance each other.

The solution of Eq. (18) is referred to as the ion-ion hybrid (or Buchsbaum) resonance

$$\omega_\mathrm{IIH}^2 = \frac{\omega_{p1}^2\omega_{c2}^2 + \omega_{p2}^2\omega_{c1}^2}{\omega_{p1}^2 + \omega_{p2}^2}. \quad (19)$$

One can show that the ion-ion hybrid resonant frequency is bounded between the two ion cyclotron frequencies, $\min(\omega_{c1}, \omega_{c2}) < \omega_\mathrm{IIH} < \max(\omega_{c1}, \omega_{c2})$. The most successful ICRF heating scenario – minority ion heating – relies on wave absorption by a small fraction of resonant minority ions (e.g, H) in deuterium majority plasmas (minority and majority ions should have different q/m). If the concentration of minority ions is much less than the concentration of majority ions, then $\omega_\mathrm{IIH} \approx \omega_{c,\mathrm{mino}}$.

Wave absorption by ions occurs in the vicinity of the ion cyclotron fundamental resonance ($\omega = \omega_{ci}$) and harmonic ($\omega = N\omega_{ci}, N \geq 2$) layers. The latter is a finite-Larmor-radius effect and usually requires significant plasma beta and pre-heating to become efficient. Since the magnetic field in tokamaks is inversely proportional to the distance to the torus axis, $B(R) \simeq B_0 R_0/R$, the lines of the ion cyclotron resonance are (almost) vertical lines in (R, Z) plane and can be determined from the following simple equation:

$$R_\mathrm{IC}\Big|_{\omega = N\omega_{ci}} \approx R_0\,(N \times Z_i/A_i)\,\frac{15.2\ B_0(\mathrm{T})}{f(\mathrm{MHz})} \quad (20)$$

($N = 1$ for the fundamental resonance, and $N \geq 2$ for harmonic resonances). Figure 5 shows the location of the ion cyclotron resonances in ITER-like plasma

for the wave frequency $f = 50$ MHz ($B_0 = 5.3$ T, $R_0 = 6.2$ T). Note that the cyclotron resonance of $^3He^{2+}$ ions is located at $R \approx 6.8$ m. It can be easily shifted to the plasma center for core ion heating by adopting a different wave frequency $f = 54$ MHz.

Frequencies used for ICRF heating in present-day fusion devices usually vary from 20 MHz to about 100 MHz, depending on the central magnetic field and ion species used for plasma heating. Note that – unlike gyrotrons – ICRF generators are much more flexible in varying wave frequency, and at every device a number of different wave frequencies are normally available for plasma heating. For instance, A2 ICRF antennas on JET have been designed to operate within the frequency range $f = 23 - 55$ MHz. For ITER, the bandwidth $f = 40 - 55$ MHz has been chosen.

iii) LH (lower hybrid), $f = f_{\rm LH}$, $f_{ci} \ll f_{\rm LH} \ll f_{ce}$.

In the intermediate frequency range between the ion and electron cyclotron frequencies, $\omega_{ci} \ll \omega \ll \omega_{ce}$, there exists another solution of Eq. (15):

$$S(\omega) = 1 - \sum_i \frac{\omega_{pi}^2}{\omega^2 - \cancel{\omega_{ci}^2}} - \frac{\omega_{pe}^2}{\cancel{\omega^2} - \omega_{ce}^2} = 0. \qquad (21)$$

For this frequency range, one can neglect ω_{ci}^2 in the denominator of the second term and ω^2 in the denominator of the third term. The corresponding solution of Eq. (21) is known as the lower hybrid resonance

$$\omega_{\rm LH}^2 = \frac{\sum_i \omega_{pi}^2}{1 + \omega_{pe}^2/\omega_{ce}^2}. \qquad (22)$$

If the second term in the denominator of Eq. (22) is much larger than one (case often relevant for astrophysical plasmas), then $\omega_{\rm LH} \approx \sqrt{\omega_{ci}\omega_{ce}}$. The LH heating utilizes the frequency range $f \approx 1-8$ GHz and is mainly used for non-inductive current-drive.

Another important factor, which influences the wave damping strength, is the wave polarization. For cyclotron resonance heating, a strong wave absorption requires a presence of the wave electric field component, which rotates in the same sense as ions for ICRF heating, and as electrons for ECRF heating. In inhomogeneous plasmas (which is the case for toroidal plasmas since B and n_e vary with the radial coordinate) – in addition to resonant frequencies – there can be cutoff frequencies (defined as $n(\omega_{\rm cutoff}) = 0$), where the incoming wave is partially reflected. Furthermore, plasmas support at least two different modes at the same wave frequency, and there are special cases, when one wave mode can be transformed into another mode with a different dispersion relation. This phenomenon is called as mode conversion and has been also actively exploited for efficient RF heating.

IV. FURTHER READING

This note is complementary to the more detailed lectures on NBI and fast-particle heating [3], and RF heating [10, 13] of the CMSS12. A comprehensive introduction to the physics of plasma heating can be found in books [1, 2]. Articles [9] and [17, 18] are focused on a discussion of heating systems of ITER and JET tokamaks. For an in-depth discussion on plasma waves, books [15, 16] are recommended.

REFERENCES

1. J. Wesson, "Tokamaks" (Oxford: Clarendon) (2004).
2. J. Freidberg, "Plasma Physics and Fusion Energy" (Cambridge University Press) (2007).
3. R. Koch and D. Van Eester, "Fast particle heating", these proceedings.
4. C.F. Barnett, "Atomic Data for Fusion, vol. 1, Collisions of H, H_2, He and Li Atoms and Ions with Atoms and Molecules", Report ORNL-6086 (1990).
5. D. Ćirić et al., *Fusion Engineering and Design* **86**, 509–512 (2011).
6. R. McAdams, "Beyond ITER: Neutral beams for a demonstration fusion reactor (DEMO)", *Review of Scientific Instruments* **85**, 02B319 (2014).
7. R. Hemswoth et al., "Status of the ITER heating neutral beam system", *Nuclear Fusion* **49**, 045006 (2009).
8. R.K. Janev, C.D. Boley and D.E. Post, "Penetration of Energetic Neutral Beams into Fusion Plasmas", *Nuclear Fusion* **29**, 2125–2140 (1989).
9. ITER Physics Expert Group on Energetic Particles, Heating and Current Drive, *Nuclear Fusion* **39**, 2495–2539 (1999).
10. E. Westerhof, "Electron cyclotron waves", these proceedings.
11. P. Dumortier and A.M. Messiaen, "ICRH Antenna Design and Matching", these proceedings.
12. F. Louche and R. Koch, "The Coupling of Electromagnetic Power to Plasmas", these proceedings.
13. R. Koch, "The ion cyclotron, lower hybrid and Alfvén wave heating methods", these proceedings.
14. D. Van Esster and E. Lerche, "Kinetic Theory of Plasma Waves", these proceedings.
15. T.H. Stix, "Waves in Plasmas" (New York: AIP) (1992).
16. M. Brambilla, "Kinetic Theory of Plasma Waves – Homogeneous Plasmas" (Oxford: Clarendon) (1998).
17. J.-M. Noterdaeme et al., *Fusion Science and Technology* **53**, 1103–1151 (2008).
18. M.-L. Mayoral et al., *Nuclear Fusion* **54**, 033002 (2014).